Nanoscale

PAPER

View Article Online
View Journal | View Issue

Cite this: *Nanoscale*, 2014, **6**, 13613

Laser-scribed graphene presents an opportunity to print a new generation of disposable electrochemical sensors†

Katie Griffiths,[a] Carl Dale,[a] John Hedley,[b] Matthew D. Kowal,[c] Richard B. Kaner[c] and Neil Keegan*[a]

Received 25th July 2014,
Accepted 22nd September 2014

DOI: 10.1039/c4nr04221b

www.rsc.org/nanoscale

Graphene application within electrochemical sensing has been widely reported, but mainly as a composite, which adds summative effects to an underlying electrode. In this work we report the use of laser-scribed graphene as a distinct electrode patterned on a non-conducting flexible substrate. The laser-scribed graphene electrode compared favourably to established carbon macroelectrodes when evaluating both inner sphere and outer sphere redox probes, providing promise of extensive utility as an electrochemical sensor. The laser-scribed graphene electrode demonstrated the fastest heterogeneous electron transfer rate of all the electrodes evaluated with a k^0 of 0.02373 cm s^{-1} for potassium ferricyanide, which exceeds commercially available edge plane pyrolytic graphite at 0.00260 cm s^{-1}, basal plane pyrolytic graphite at 0.00033 cm s^{-1} and the very slow and effectively irreversible electrochemistry observed using single layer graphene. Finally and most significantly, a proof of principle system was fabricated using the laser-scribed graphene as working electrode, counter electrode and underlying base for the Ag/AgCl reference electrode, all *in situ* on the same planar flexible substrate, removing the requirement of macroscale external electrodes. The planar three electrode format operated with the same optimal electrode characteristics. Furthermore, the fabrication is inexpensive, scalable and compatible with a disposable biosensor format, considerably widening the potential applications in electrochemical bio-sensing for laser-scribed graphene.

Introduction

A diverse range of chemical and biochemical analytes have been detected using carbon materials as electrodes, or components of electrodes, in electrochemical assays. The composition of carbon electrodes used in electrochemistry are highly heterogeneous in nature with examples including glassy carbon,[1] carbon paste,[2] screen printed carbon,[3] edge-plane pyrolytic graphite (EPPG)/basal-plane pyrolytic graphite (BPPG),[4,5] carbon nanotubes[6] and graphene.[7] Interestingly, the electron transfer rate and analytical performance of these electrodes are dramatically influenced by the structural nature of the carbon material itself, which is largely due to differences in the density of electronic states and edge-plane sites available on the carbon electrode surface.[8] This is well demonstrated by the now common method of modifying underlying carbon electrodes with carbon nanotubes, engendering enhanced electrochemical performance. The original demonstration was performed by Wang's group who discovered the addition of carbon nanotubes allowed a large reduction in the overpotential for NADH detection compared with unmodified glassy carbon electrodes.[6] In further work, Wang's group used multi-walled carbon nanotubes as the underlying electrode by screen printing them as an ink, which gave increased current densities and reduced overpotentials for numerous electroactive species compared with a commercial carbon ink.[9] However, a fundamental observation by Compton's group is worth bearing in mind. The electro-catalytic performance reported for carbon nanotubes should be substantiated using the relevant controls when modifying a pre-existing electrode, for example, substituting carbon nanotubes for graphite powder.[10] In fact, the same group wrote two illuminating and extensive reviews advocating that EPPG electrodes were often advantageous over carbon nanotubes and other carbon based electrodes in electrochemical sensing, due to the increased

[a]*Institute of Cellular Medicine, Newcastle University, Newcastle upon Tyne, NE2 4HH, UK. E-mail: Neil.Keegan@newcastle.ac.uk; Fax: +44 (0)191 2087991; Tel: +44 (0)191 2083678*
[b]*School of Mechanical and Systems Engineering, Newcastle University, Newcastle upon Tyne, NE1 7RU, UK*
[c]*Department of Chemistry and Biochemistry, University of California, Los Angeles (UCLA), Los Angeles, California 90095, USA*
† Electronic supplementary information (ESI) available. See DOI: 10.1039/c4nr04221b

edge plane/defect sites they possess.[4,5] It appears likely that EPPG has been sidelined to academic endeavours due to the manufacturing route and operation. It is cut from highly ordered pyrolytic graphite and housed in an external casing before operation using macroscale external reference and counter electrodes, making commercial exploitation problematic due to difficulties in mass production and miniaturisation. In contrast, screen printed carbon electrodes heralded a turning point in mass production of whole systems for numerous electrochemical sensing applications, utilising in-built reference and counter electrodes on a planar substrate, ultimately producing a notable commercial success, namely the multi-billion dollar glucose sensor.[3] Any material that can be very simply printed with properties akin to, or even better than EPPG should be very appealing.

Considering the rich history of carbon based materials in electrochemical sensing it is hardly surprising that graphene has become a focal point of electrochemical research over recent years. Graphene in its truest form represents a single, or few layers of carbon in an atomic scale honeycomb lattice (an unrolled carbon nanotube), as per the 2004 seminal experiments performed by Geim and Novoselov.[11] Even within the landscape of ongoing materials optimisation using numerous alternative processing routes,[11–14] the scientific community has revealed many advantageous properties for the emergent material, such as high thermal conductivity, mechanical strength and unique electronic properties.[15] In contrast, the fundamental electrochemical properties of graphene are not deciphered to the same degree as its electronic properties. This is hardly surprising as the plethora of scientific literature on graphene electrochemistry actually revolves around solution miscible graphene derivatives that are easier to produce, such as graphene oxide (GO),[16] which can be chemically,[17,18] thermally,[19] or electrochemically[20] reduced to generate structure and properties similar to pristine graphene. The reduced graphene oxide will inevitably still contain numerous defect sites, but in electrochemistry this can be very advantageous regarding heterogeneous electron transfer, which will mainly occur at edge-plane defect sites.[21] The solution miscible graphene derivatives are predominantly drop-cast onto underlying electrodes – in essence the graphene derivatives are acting in concert with the underlying electrode – producing summative electrochemical effects.[18–21]

Papers that use graphene as the standalone electrode have been published, but such studies are sparsely represented. One example showed that an epitaxial graphene electrode required significant anodisation to improve on poor initial electrochemical behaviour towards the inner sphere redox couple potassium ferricyanide.[22] However, the redox electrochemistry of monolayer CVD graphene towards the outer sphere redox couple ferrocenemethanol was demonstrated to be ten-fold faster than basal plane pyrolytic graphite.[23] A subsequent paper using monolayer CVD graphene as the electrode concluded that CVD graphene was akin to EPPG with regard to simple biological redox couples, while biological analytes that require surface oxygen species to act as adsorption mediators show poor electrochemistry compared to EPPG. The authors concluded that a pristine graphene electrode should be akin to BPPG electrodes, which lacks edge sites for superior electrochemistry and that graphitic islands within their layers may be responsible for the results.[24] In fact, the same group was even more conservative in a paper directed at a fundamental examination of graphene as an electrochemical sensing material. Here they concluded that flakes of pristine graphene monolayers deposited on an EPPG electrode block electron transfer from solution to the electrode and increase the peak to peak separation (ΔE_p) of the underlying EPPG electrode. In short, the conclusion was that the edge- to basal-plane ratio is critical, so a true monolayer of pristine graphene would possess a low concentration of edge-plane sites, exhibiting poor electrochemical behaviour in response to many analytes of interest.[25] The theoretical and experimental conjectures surrounding pristine graphene in a continuous layer seem reasonable and follow the accepted view that carbon materials with a basal-plane structure will have a low density of states and sparcity of surface adsorption sites for electron transfer from the solution phase,[8] but the empirical results have been slightly better than one would expect, which could be due to the overall quality of the starting material.

Interestingly, the fabrication of laser irradiated reduced graphite oxide films as standalone electrodes were demonstrated as a route to fabrication of super-capacitors in 2011.[26] This was followed by simplification of the laser source and generation of laser-scribed graphene (LSG) as a new member of the graphene family, which is produced by thermally reducing a film of graphite oxide at predefined positions using a LightScribe DVD burner.[27,28] The laser-irradiated graphite oxide areas were very effectively reduced demonstrating a rapid expansion and exfoliation of the layers, producing a film with excellent conductivity, high porosity and providing a surface area of 1520 $m^2\ g^{-1}$.[27,28] The rapid exfoliation and increase in surface area is indicative of the graphene layers existing as individual monolayers with limited restacking into graphitic sheets.[27] The reduction process also drastically altered the films C/O ratio finishing with a carbon content of 96.5% and residual oxygen content of 3.5%.[26] Laser-scribed graphene has already demonstrated promise in super-capacitors,[28] gas sensors[27] and more recently strain sensors.[29] The LSG gas sensor work also discusses the possibility that the LSG material should have a high degree of edge plane content, which would open up many avenues of research regarding electrochemical biosensors.[27]

The current work validates previous physicochemical characterisation of laser-scribed graphene and performs an in-depth study of the utility of laser-scribed graphene as an electrochemical transducer. The LSG fabrication method allows the facile production of scalable and flexible electrochemical sensors whose electrodes are made exclusively of graphene with no underlying electrode material and no added composites. The study uses well-characterised inner sphere and outer sphere redox couples to probe the properties of LSG and benchmarks performance against various all-carbon

electrodes, including EPPG, BPPG and monolayer CVD graphene. In the initial experiments 3 mm diameter LSG working electrodes were used in conjunction with macroscale external reference and counter electrodes. However, in the final experiments the LSG fabrication process was used to produce a planar three electrode system consisting of an all-graphene working electrode, counter electrode and a graphene base for the simple Ag/AgCl reference electrode. The whole process was accomplished without the requirement of lithographic masks or photoresist.

Results and discussion

Physicochemical characterisation of laser-scribed graphene electrodes

The LSG electrodes were fabricated at wafer level using the LightScribe DVD label writing technology and a GO film to produce individual LSG electrode devices. The LightScribe technology allows direct laser writing of DVD labels into user-defined designs by utilising the same drive that writes the data. In short, the process is adopted so that the laser thermally reduces an insulating GO film at predefined positions programmed into the software, thus creating bespoke conducting LSG electrodes. A schematic of the process can be seen in Fig. 1A in which a polyethylene terephthalate (PET) film allows flexible handling of the devices for ease of packaging. This one-step patterning process can be carried out in any lab with basic computer facilities and requires no masks for fabrication, or expensive lithography, which are required for screen-printed and microfabricated electrochemical sensors, respectively. Scanning electron microscopy images of the LSG surfaces were in line with previous literature that states the stacked graphite oxide sheets undergo rapid thermal shock on laser ablation causing reduction, exfoliation and expansion of the film indicative of graphene sheets, which do not restack.[27–29] Fig. 1B shows that the thermal reduction induces a large scale expansion on the LSG area as opposed to the original GO film. Across the samples the expanded LSG height was approximately 10 μm, this is qualitative as the SEM images were tilted, but is in fair agreement with the previous literature at 7.6 μm.[28] Cross-sections of the GO film and LSG material are clearly indicative of the chemical change from stacked graphitic sheets in the GO film (Fig. 1C) to an unordered network structure with a high edge plane content in the LSG film (Fig. 1D). The sheet resistance of the graphite oxide film in this study was essentially insulating at 13.6 MΩ sq^{-1} while the laser reduction process produced a LSG sheet resistance of 589 Ω sq^{-1}. This transformation into a conductor is in agreement with the earlier report by Strong *et al.*[27] which stated a sheet resistance value of 80 Ω sq^{-1} for LSG, significantly reduced from that of the GO film at more than 20 MΩ sq^{-1}. Raman spectroscopy of the layers in a previous study by the Kaner group detailed the effectiveness of the process in controllably producing few layer laser-scribed graphene with high edge plane content.[27] In our study, the oxygen/carbon ratio was used as a quality control method to ensure the reduction process was effective and X-ray photoelectron spectroscopy (XPS) analysis was performed to this end. Fig. S1† shows the oxygen content is reduced from 42.4% in the GO film to 6.5% in the LSG film immediately after the thermal reduction process, thus confirming the effective reduction of oxygen and a return to the sp^2 bonded carbon structure across the basal plane of the individual few layer graphene sheets. This level of oxygen content is known to be advantageous for numerous electrochemical redox reactions that are termed inner sphere, due to their reliance on surface species such as oxygen derived functional groups to aid electron transfer at the electrode surface.[8] Ultimately, the prevalence of edge plane content within LSG electrodes should compare favourably with existing state-of-the-art carbon electrodes whilst offering the advantage of scalable cost effective manufacture. To evaluate this hypothesis, both inner and outer sphere redox reactions were analysed using single LSG working electrodes in conjunction with external reference and counter electrodes. The electrochemical performance was compared with established carbon electrodes and single layer graphene (SLG).

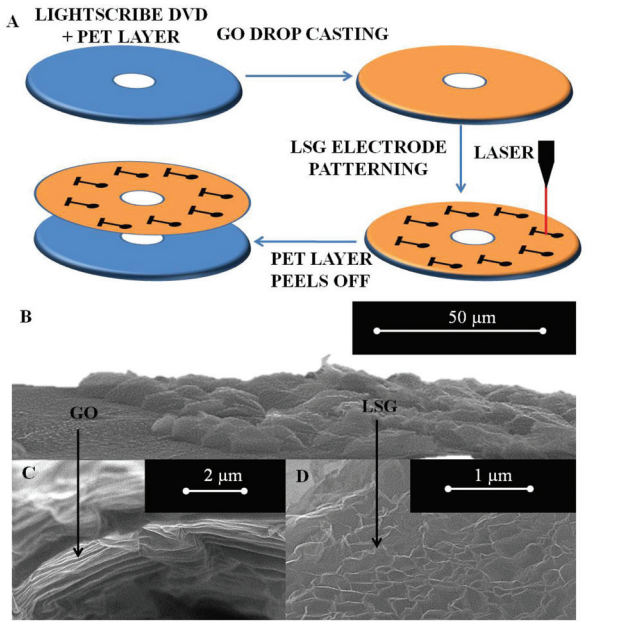

Fig. 1 Panel (A) shows the overall process of patterning LSG electrodes on a flexible PET substrate. Panel (B) shows a SEM image directly contrasting the initial GO film with a LSG area, which demonstrates that laser-irradiation produces characteristic exfoliation of the layers and increased surface area. Panel (C) shows a magnified image of a GO cross section clearly visualising flat stacked layers. Panel (D) shows a magnified image of a LSG cross section visualising the formation of an expanded network structure with high edge plane content.

Electrochemical sensing of inner- and outer-sphere redox probes using LSG electrodes

Cyclic voltammetry (CV) was used for electrode characterisation. CV potential forward and reverse scans were performed with respect to a standard Ag/AgCl reference electrode and

platinum counter electrode unless otherwise stated. A photograph of the LSG electrode set-up can be seen in Fig. S2† panel A. A range of carbon-based electrodes were selected for comparison with LSG electrodes and the diameter of the working electrode standardised at 3 mm. EPPG was chosen as the gold standard comparator, as it has good heterogeneous electron transport rates as a consequence of its high proportion of edge plane sites. BPPG was selected as a comparator due to the multitude of examples in the literature that demonstrate reduced electrode performance due to its lack of oxygen defects and edge plane sites as compared to EPPG.[27] Finally, SLG electrodes were investigated to assess the benefits of using the network structure of LSG over the pristine single layer graphene structure. First, CVs were performed in 1,1′-ferrocene dimethanol, an outer-sphere redox species, insensitive to surface oxides. The response was thus solely dependent upon density of states (DOS). Second, experiments were conducted in potassium ferricyanide, an inner-sphere redox species that is known to be sensitive to surface oxides.[8]

In 1,1′-ferrocene dimethanol, the BPPG electrodes demonstrated the lowest peak potentials and LSG produced the greatest peak currents of all the electrodes tested, as seen in Fig. 2A. Table 1 details the comparative electrochemical parameters taken from the scans. The peak separation for the LSG, EPPG and the BPPG remained close to the 59 mV theoretical ideal for a one electron transfer process, with a ΔE_p, of 54 mV, 58 mV and 59 mV, respectively. The SLG performance was poor in comparison to the pyrolytic graphite and LSG in terms of peak current response. In addition, the ΔE_p of SLG was also inferior with a peak separation of 79 mV, which is suggestive of a much slower electron transfer rate. Interestingly, previous reports have commented on the presence of graphitic islands in commercially available graphene samples providing better than expected SLG electrochemistry;[24] whereas our SLG samples appear to be very high quality, as detailed in Raman spectra found in Fig. S3.†

Fig. 2B shows the various electrochemical responses for the inner-sphere redox probe potassium ferricyanide. Interestingly, the SLG provides an extremely poor electrochemical response; it presents lower peak currents than LSG, EPPG and BPPG, while the peak separation is essentially irreversible in the window measured, which is indicative of a very slow heterogeneous electron transfer rate. However, this is hardly surprising considering the theoretical structure of pristine graphene with its low edge and oxygen content, which is far from ideal for an inner-sphere redox probe electron transfer rate. Our results are in line with Brownson *et al.*, who demonstrated that higher quality SLG electrodes have a very poor electrochemical response towards inner-sphere redox probes, with a quoted ΔE_p of 1242.7 mV (at 100 mV s^{-1}).[30] The clear trend is that SLG performed poorly and is at best analogous to BPPG.

In contrast, the LSG electrode demonstrates high current densities, low overpotentials and the smallest peak separation with a ΔE_p of only 59 mV compared with the 85 mV of EPPG and 176 mV for BPPG. This clearly demonstrates the superior

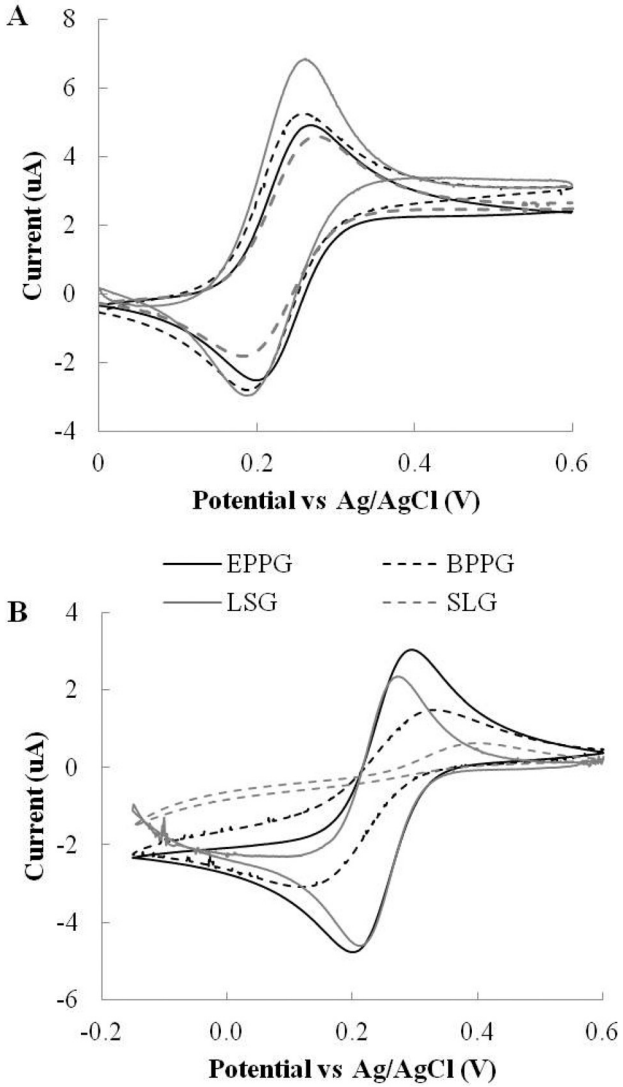

Fig. 2 Cyclic voltammograms of (A) 1,1′-ferrocene dimethanol and (B) potassium ferricyanide in 1 M KCl at a scan rate of 10 mV s^{-1} at unmodified 3 mm diameter EPPG, BPPG, LSG and SLG electrode surfaces.

Table 1 ΔE_P values for selected electrode materials

Electrode material[a]	ΔE_P/mV in 1,1′-ferrocene dimethanol	ΔE_P/mV in potassium ferricyanide
EPPG	58	85
BPPG	59	176
SLG	79	NA[b]
LSG average (n = 4)	54	59
RSD	5.5%	5.1%

[a] Two redox species were investigated, 1,1′-ferrocene dimethanol and potassium ferricyanide. Results of four LSG electrodes are presented to confirm reproducibility of the ΔE_p with this new material. [b] SLG did not demonstrate a reversible redox reaction with potassium ferricyanide and so a ΔE_P could not be determined.

Table 2 Electrochemical parameters of four LSG electrodes[a]

		E_{pa} (V)	i_{pa} (μA)	E_{pc} (V)	i_{pc} (μA)
1,1′-Ferrocene dimethanol	1	0.199	−4.634	0.256	6.523
	2	0.199	−4.576	0.253	5.890
	3	0.204	−5.293	0.254	7.650
	4	0.196	−4.785	0.251	6.223
	Average	0.200	−4.822	0.254	6.572
	RSD	**1.7%**	**6.8%**	**0.8%**	**11.6%**
Potassium ferricyanide	1	0.212	−4.100	0.274	3.720
	2	0.214	−3.703	0.270	3.959
	3	0.213	−3.602	0.269	3.401
	4	0.211	−3.887	0.271	3.828
	Average	0.213	−3.823	0.271	3.727
	RSD	**0.6%**	**5.7%**	**0.8%**	**6.4%**

[a] Ferrocene dimethanol and potassium ferricyanide were used as the redox probes. For inter-reproducibility purposes the mean, and percentage relative standard deviation (RSD) are shown for four LSG electrodes with each of the redox probes assessed to confirm reproducibility of electrochemical responses with this new material.

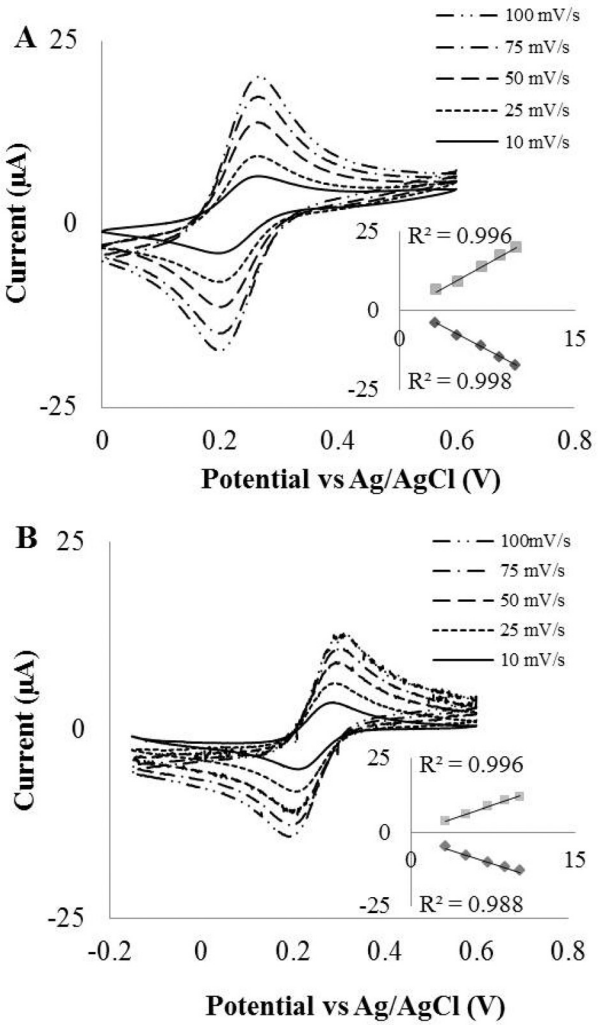

Fig. 3 Effect of scan rate on peak current and peak potential for LSG electrodes in 1,1′-ferrocene dimethanol (A) and potassium ferricyanide (B). Inset shows that peak current is proportional to square root of scan rate. Scans were performed at 10, 25, 50, 75, 100 mV s^{-1}.

electrochemical response of LSG even compared with EPPG, the gold standard of carbon electrodes, likely due to an optimal O/C content and accessibility to many edge sites at the electrodes surface. The inner sphere redox probe clearly shows the difference in electrochemical performance of EPPG and BPPG, where the ΔE_p of the BPPG (176 mV) is now more than double that of the EPPG (85 mV) with severely decreased peak current responses due to its basal plane configuration.

These data clearly establish that the LSG electrodes perform better/on par with EPPG for inner-sphere and outer-sphere redox probes. The performance is noteworthy as the LSG electrode is not a composite, unlike the vast proportion of the reduced graphite oxide (rGO) electrodes cited in the literature, which require an underlying electrode, such as glassy carbon.[31–37] The results of the electrochemical studies of LSG along with the XPS analysis (Fig. S1†) suggest that the material offers an optimal balance of oxygenated edge defects. This allows efficient heterogeneous electron transfer, while maintaining a high level of electrical conductivity, resulting in a highly effective electrode.

Inter-reproducibility of the Laser-Scribe method of electrode manufacture was then assessed. Again, using the inner- and outer-sphere redox probes potassium ferricyanide and 1,1′-ferrocene dimethanol, the peak potential (E_p) and peak current (i_p) were determined for each of four electrodes. The results are presented in Table 2. The relative standard deviation of the anodic and cathodic peak current response were generally good providing an acceptable level of reproducibility. The relative standard deviation of the E_p was of particular note as all values are well below 2% suggesting that the electrodes have huge potential for specific detection of redox species in voltammetric applications.

Next, the effect of scan rate on the behaviour of LSG electrodes was considered (Fig. 3). Both the inner- and outer-sphere redox species discussed earlier were used and CVs were performed at scan rates varying from 10 to 100 mV s^{-1}. The peak current responses were proportional to the square root of the scan rate in both, as shown in Fig. 3 inset, suggesting a diffusion-controlled voltammetry response. However, the behaviour of peak separation varied between the two redox species. In 1,1′-ferrocene dimethanol the ΔE_p remains close to the theoretical value even with an increased scan rate, but for the potassium ferricyanide the ΔE_p widens with increasing scan rate resulting in quasi-reversible behaviour. The rate constant is lowered due to the equilibrium at the surface being reached more slowly and therefore, an increase in scan rate causes a shift in peak potentials. The scans performed in potassium ferricyanide also demonstrate a quasi-reversible process with EPPG and BPPG (data not shown). Using these data the electrode reaction kinetics can be calculated utilising the Nicholson method.[39] This allows a direct comparison of LSG with EPPG and BPPG under identical experimental conditions. In order to calculate an estimate of the heterogeneous

electrochemical rate constant k^0, the dimensionless kinetic parameter Ψ was first determined from the equation.[40]

$$\Psi = (-0.6288 + 0.0021X)/(1 - 0.017\ X)$$

where X was equal to the peak potential separation (ΔE_p) of the system multiplied by the number of electrons involved in the electrochemical reaction (n), which in the case of the potassium ferricyanide reaction was equal to one. Following the calculation of Ψ the k^0 could be determined using the equation[39,40]

$$\Psi = k^0[\pi DnvF/(RT)]^{-1/2}$$

where D was the diffusion coefficient of the oxidation of the electroactive species, v is the scan rate in V s^{-1}, F is the Faraday constant, R is the universal gas constant and T the absolute temperature. The diffusion coefficient was approximated to be 5.4×10^{-6} cm^2 s^{-1} for potassium ferricyanide, as used by Valota *et al.* in the investigation of electrochemical performance of monolayer and bi-layer graphene.[41] Thus, in 1 mM potassium ferricyanide the k^0 of LSG was calculated as 0.02373 cm s^{-1}, demonstrating a favourable electron transfer rate when compared with EPPG at 0.002601 cm s^{-1} and BPPG 0.00033 cm s^{-1}. The order of magnitude difference between the EPPG and BPPG is to be expected due to the availability of defect sites being significantly greater at the edge-plane than at the basal-plane of pyrolytic graphite. What is interesting is that the k^0 of LSG is significantly increased compared with EPPG, further evidencing the practicality of this material for electrochemical biosensors. The results shown here are given further credence and show the same trend as a recent paper investigating Q-graphene and the beneficial effect it had on the electrochemical response of EPPG electrodes.[38] The k^0 of potassium ferrocyanide(II) on EPPG was shown to be 0.00466 cm s^{-1}, but it underwent a significant increase to 0.0186 cm s^{-1} when the electrode was modified with Q graphene. The LSG is clearly showing strikingly similar advantages to the work carried out by Randviir *et al.*[38] but our work is a standalone electrode with no additive effects and is clearly applicable to facile scalable mass production unlike previous work.

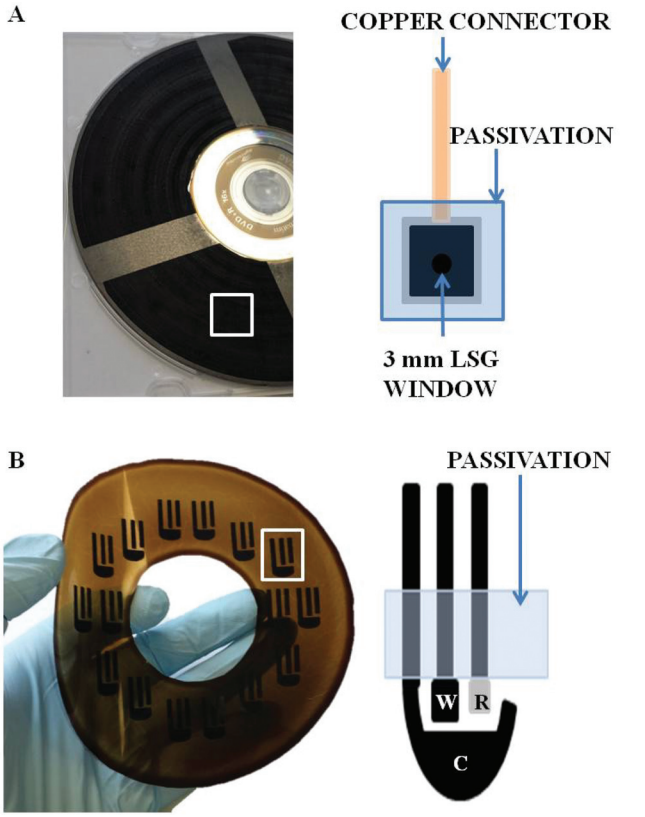

Fig. 4 Panel A shows an entire disc coated in GO and scribed to produce large scale sections of LSG (clear contrast can be seen between the black LSG sections and silver GO sections). Electrodes were then cut from the LSG on the flexible substrate. Electrical connections were made with conductive copper tape and the electrode was then passivated leaving only a 3 mm diameter window for electrochemical reactions to occur at the LSG surface. This electrode could be used with macroscale external reference and counter electrodes. Panel B shows patterned LSG electrodes forming the basis of a planar three-electrode system for electrochemical analysis without the need for an external reference and counter electrode. The schematic to the right shows the LSG working electrode (W), LSG counter electrode (C) and the reference electrode (R) which is silver adhesive paint manually applied to a LSG base.

Electrochemical evaluation of a planar three-electrode LSG system

In the initial characterisation study LSG electrodes were constructed as individual working electrodes, as shown in Fig. 4A, using conventional external reference and counter electrodes. The second aim of our study was to assess the possibility of not only having a stand-alone graphene electrode, but to incorporate that electrode into a fully disposable planar three-electrode system that requires no external reference, or counter electrode, as depicted in schematic Fig. 4B and a photograph in Fig. S2† panel B. Effectively, this is wafer level production of a planar printed three-electrode system, akin to screen printing, or microfabrication of conventional materials such as carbon paste and gold, but updated to utilise mask-free generation of LSG. The GO, which undergoes no thermal patterning and modification, retains its insulating properties, so it can remain *in situ*. Silver was applied to the third electrode which acted as a Ag/AgCl reference electrode and the larger LSG electrode was used as a counter electrode. In this work the silver paint was applied by hand and no masking steps were used, although there are many alternative routes, for example electroplating. Pseudo-reference electrodes are often variable in their performance compared with a standard silver/silver chloride reference electrode, which contains a liquid double junction and inner solution saturated with KCl. However, our pseudo-reference electrode potential only varied from the standard reference electrode potential between 0.99 mV to −1.97 mV in 1,1′-ferrocene dimethanol and 0.60 mV to −4.59 mV in potassium ferricyanide. Hence the voltammetric responses recorded below remain at a similar potential for the

pseudo-reference electrode as compared to the standard silver/silver chloride reference electrode and the differences are essentially within the experimental error.

The electrochemical performance of the LSG planar three-electrode system is shown in Fig. 5 compared with EPPG (the EPPG has macroscale external reference and counter electrodes). It can be seen that when performing CVs in ferrocene dimethanol, the LSG planar three-electrode system performs comparably with the EPPG, the gold standard of carbon electrodes as discussed at length previously in this work. Interestingly, the LSG sensor demonstrates lower peak potentials suggesting that it may be useful in the detection of biological molecules since detection at lower potentials decreases the likelihood of electrochemical interference. Both electrode materials demonstrate a Nernstian response with ΔE_p values of 57 mV and 58 mV for LSG and EPPG, respectively. Using the potassium ferricyanide redox probe, the LSG sensor is shown to have a ΔE_p of 75 mV, which compares favourably with the 85 mV achieved with the EPPG. The potassium ferricyanide ΔE_p value for the planar three electrode system is slightly altered from the external reference electrode system at 59 mV (Table 1). A possible explanation for this was investigated using a new batch of graphite oxide and two additional LSG processing runs. Representative potassium ferricyanide CV scans can be seen in Fig. S4† generating a ΔE_p value of 63 mV for the stand-alone LSG electrode and 61 mV for the planar three electrode LSG system, which is in excellent agreement with the original reproducibility data in Table 1. It would appear that a subtle change in the electrode processing, most plausibly the surface oxygen content, has marginally altered the electrode performance towards the inner sphere redox probe in Fig. 5. This highlights the possibility of minor processing differences between batches, however, the effect is minimal, and indeed potassium ferricyanide is well known to be very sensitive to small changes in surface species,[8] so the spread of results between batches, as well as within a batch is very small. It is worth noting that the LSG outperformed the EPPG regarding all potassium ferricyanide results. Representative scans of 1,1′-ferrocene dimethanol can also be found in Fig. S4† using the two additional processing runs. The ΔE_p values of 54 mV and 60 mV were achieved with the stand-alone LSG electrode and the planar three electrode LSG system respectively, which compares well with the results shown in Table 1 for 1,1′-ferrocene dimethanol. These data further demonstrate the reproducible nature of the LSG electrodes between processing runs as well as within a processing run (Table 1). Ultimately, the LSG three-electrode system is equivalent to, or arguably marginally outperforms, EPPG in terms of peak current response, peak potential and ΔE_p. Most importantly, EPPG will always need a macroscale cut from highly ordered pyrolytic graphite and macroscale external reference/counter electrodes, which are not compatible with mass production. LSG on the other hand is clearly suitable to scalable, inexpensive mass production in a planar three-electrode configuration, which has seen great commercial success in the past using the classical techniques of screen printing and microfabrication. Parallel processing in microfabrication/screen printing would still be superior to a single DVD drive, where the processing, although producing multiple devices, could be thought of as serial in nature. However, due to the attributes of computer technology it is conceivable that a manufacturer could stack hundreds of DVD writers to fabricate LSG devices in a highly parallel manner.

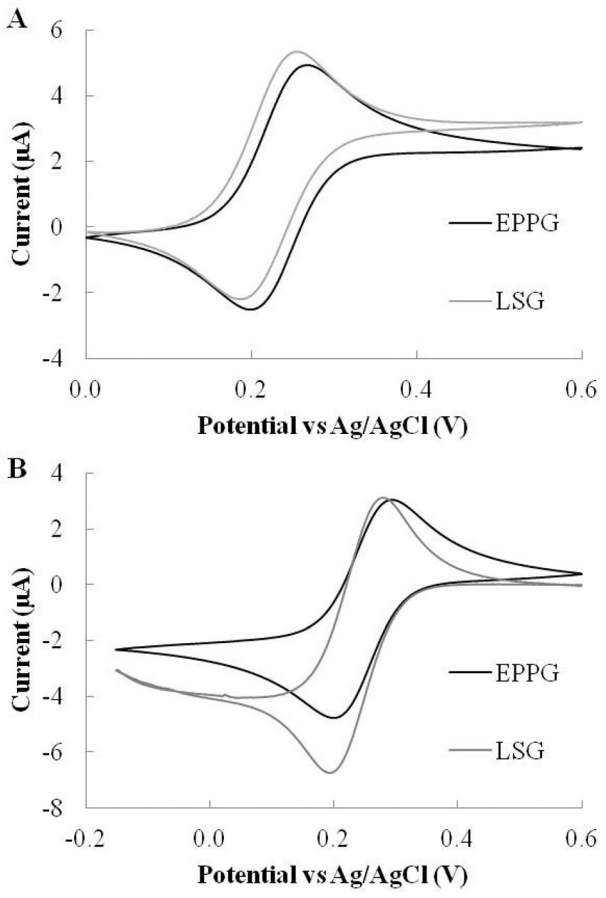

Fig. 5 Panel A shows cyclic voltammograms of 1,1′-ferrocene dimethanol and panel B potassium ferricyanide at a scan rate of 10 mV s^{-1} at EPPG electrode surfaces compared to the disposable planar three electrode LSG system.

Conclusions

The electrochemical behaviour of LSG has been methodically investigated as a stand-alone electrode by comparing it with highly relevant carbon alternatives, EPPG, BPPG and SLG. Interestingly, SLG performs very poorly with regard to the electrochemical response to both inner- and outer-sphere redox couples, which is in line with an observation made in a 2014 publication[29] and also the theory regarding a defect-free basal-plane structure.[8] This is important in its own right as graphene used in electrochemical sensing has been widely reported, but in most cases has only been successful as a composite. The graphene flakes seemingly improve the underlying

electrodes due to the addition of favourable carbon architectures with a large number of edge plane sites and some degree of surface oxygenation.[38] In this study we clearly show that the LSG electrode displays the optimal surface qualities for electrochemistry, in its own right without summative effects, as it compares favourably to the referee carbon electrode, EPPG, in terms of peak current response, ΔE_p and heterogeneous electron transfer rates. This dovetails nicely with empirical evidence that the LSG material can be fabricated as a disposable sensor, in a planar three-electrode system, with no loss of performance. The LSG performance, inter-electrode reproducibility and amenability to a disposable format will open up many potential opportunities in the electrochemical bio-sensing arena and the authors are now investigating the material with respect to biological systems.

Experimental

Materials

Chemicals were purchased from Sigma-Aldrich and were analytical grade unless otherwise stated. Potassium ferricyanide and 1,1′-ferrocene dimethanol were used as inner- and outer-sphere redox probes at 1 mM in 1 M KCl as supporting electrolyte.

Graphene oxide (GO) was prepared using a modified Hummers method[42,43] beginning with graphite from Bay Carbon, Inc. Polyethylene terephthalate (PET, Niceday Guilbert) was used as a flexible substrate for GO and was attached to a Lightscribe DVD using SprayMount (RS Components, Northants). The HP lightscribe DVD RW drive was used with Lightscribe software for designing the laser-scribe patterns of the electrodes. Silver paint, conductive copper tape and Kapton tape were purchased from RS components (Northants). Platinum foil 99.99% trace metals basis (Sigma Aldrich) was purchased for use as a counter electrode. The Ag/AgCl reference electrode was from BASi (Indiana, USA). EPPG and BPPG electrodes (3 mm diameter) from IJ Cambria Scientific Ltd were used for comparison purposes as was CVD 1 cm^2 single layer graphene on 285 nm silicon dioxide/silicon (p-doped) (Graphene Supermarket).

Manufacture of laser-scribed graphene

The GO suspension was diluted in deionized water (dH_2O), 1.5 g of GO suspension was added to 20 ml dH_2O and sonicated at 55 °C for 90 min. The suspension was then drop-cast onto a PET covered DVD and allowed to dry overnight on a level surface. Once dry, the disc was placed label and GO side down into a Lightscribe enabled disc drive and the GO was laser reduced to the desired pattern. Each laser irradiation cycle takes 20 minutes to complete. The laser scribing procedure was repeated ten times in order to ensure maximum reduction of the GO, optimal expansion and increased conductivity. It has previously been shown that the level of laser reduction can be tuned for electrical conductivity over five orders of magnitude using one, two, or three reduction steps and the grey scale power settings, eventually saturating the attainable conductivity.[27] The number of cycles chosen reflects our wish to saturate the reduction process, but it is possible that fine tuning the oxygen content may be appropriate for specific electrochemical analysis. The LSG could then be removed from the disc on the flexible substrate and cut into individual electrodes. It is worthy of note that the resolution of the LightScribe 780 nm laser is 20 microns[44]

Laser-scribed graphene characterisation

Environmental scanning electron microscopy was performed to visualise changes in GO to LSG following laser reduction. An FEI-Philips XL30 ESEM was used to image the surface of GO and LSG. The GO and LSG films were carefully separated from the acetate substrate prior to imaging in order to reduce any charging effects.

XPS analysis of the GO and LSG was performed by NEXUS at nanoLAB (Newcastle University). Full spectrum surveys were performed as well as analysis of the C_{1S} and O_{1S} peaks at 284 eV and 532 eV, respectively. Measurements were taken at five positions across the surface of the films. Peak fitting was performed using Casa XPS in order to determine bonding configurations and carbon : oxygen changes due to the reduction by laser irradiation.

The Raman spectra were performed using a Horiba Jobin Yvon HR800 Raman spectrometer with a 532 nm excitation laser.

Laser-scribed graphene electrodes

The LSG standalone electrodes were initially prepared using a disc of GO that had been entirely laser-scribed to form a continuous surface of LSG. This sheet of LSG could then be cut to size and prepared for use as an electrode. Conductive silver paint was used in order to contact the LSG to copper tape. Contact lines of silver paint were drawn around a 1 cm^2 piece of LSG, to one edge a strip of copper foil was attached to allow contact for electrochemical measurement. The electrode was then passivated using Kapton tape, leaving only a 3 mm diameter LSG surface available for electrochemical activity as demonstrated in Fig. 4A. A similar method was used with the 1 cm^2 single layer graphene (SLG) to create a SLG electrode of 3 mm diameter for comparison.

The disposable three electrode system, including tracking for electrical connections, was produced by specifically patterning LSG on a GO covered disc by laser irradiation. The LSG working electrode was standardised to an area of 7.1 mm^2 for easy comparison to other electrodes unless otherwise stated. Once laser reduced, the three-electrode design was removed from the disc and cut to size. A copper tape contact was made to each electrode and a Ag/AgCl reference electrode was added by hand using silver paint. Chloride ions were available in the 1 M KCl supporting electrolyte. The tracking was passivated with Kapton tape leaving only the silver reference, LSG working and counter electrodes exposed, a schematic and example are shown in Fig. 4B.

Electrochemistry

A three-electrode system was employed. A platinum counter electrode was created using platinum foil, copper tape and Kapton tape to produce a platinum electrode surface of 2.5 cm^2, and a standard Ag/AgCl reference electrode was used. Carbon based working electrodes were chosen for comparative work including EPPG, BPPG and SLG. Measurements were performed with an Autolab electrochemical workstation (Ecochemie) and a general purpose electrochemical system. All electrochemistry was performed in 1 M KCl supporting electrolyte. The CV step potential was maintained at 1 mV in all experiments and a scan rate of 10 mV s^{-1} was used except when directly investigating the effect of scan rate on LSG electrodes. For each CV experiment, 5 CV scans were performed with the first being discarded to allow for equilibration at the electrode surface and therefore the mean of 4 scans was determined. Background scans in the 1 M KCl supporting electrolyte were also monitored and subtracted.

Experiments comparing the different types of working electrode were performed using 1,1′-ferrocene dimethanol and potassium ferricyanide. When using 1,1′-ferrocene dimethanol, the potential was cycled between 0.6 V and 0.0 V, while, using potassium ferricyanide, the potential was cycled between 0.6 V and −0.15 V. When investigating the effect of scan rate on the peak current and the ΔE_p, CVs were performed at 10, 25, 50, 75 and 100 mV s^{-1}.

Acknowledgements

The authors would like to thank Dr Naoko Sano at Newcastle University for help with XPS analysis, Professor Fraser Armstrong at Oxford University for supplying initial examples of EPPG macroelectrodes, Isabel Arce-Garcia for access to the ESEM at Newcastle University and Prof. Calum McNeil at Newcastle University for useful discussion. This work was funded through an EPSRC PhD studentship, EPSRC Cross Disciplinary Feasibility award (EP/I015930/1) and UKIERI Trilateral Research Partnership funding (UKIERI-TRP-2012/13-0010).

References

1 R. D. O'Neill, S. C. Chang, J. P. Lowry and C. J. McNeil, *Biosens. Bioelectron.*, 2004, **19**, 1521–1528.
2 J. Kulys, *Biosens. Bioelectron.*, 1999, **15**, 473–479.
3 M. Albareda-Sirvent, A. Merkoçi and S. Alegret, *Sens. Actuators. B*, 2000, **69**, 153–163.
4 C. E. Bank and R. G. Compton, *Analyst*, 2006, **131**, 15–21.
5 C. E. Banks and R. G. Compton, *Anal. Sci.*, 2005, **21**, 1263–1268.
6 M. Musameh, J. Wang, A. Merkoci and Y. Lin, *Electrochem. Commun.*, 2002, **4**, 743–746.
7 M. Pumera, A. Ambrosi, A. Bonanni, E. L. K. Chng and H. W. Poh, *TrAC*, 2010, **29**, 954–965.
8 R. I. McCreery and M. T. McDermott, *Anal. Chem.*, 2012, **84**, 2602–2605.
9 J. Wang and M. Musameh, *Analyst*, 2004, **129**, 1–2.
10 R. R. Moore, C. E. Banks and R. G. Compton, *Anal. Chem.*, 2004, **76**, 2677–2682.
11 K. S. Novoselov, A. K. Geim, S. V. Morozov, D. Jiang, Y. Zhang, S. V. Dubonos, I. V. Grigorieva and A. A. Firsov, *Science*, 2004, **306**, 666–669.
12 C. Berger, Z. Song, T. Li, X. Li, A. Y. Ogbazghi, R. Feng, Z. Dai, A. N. Marchenkov, E. H. Conrad, P. N. First and W. A. de Heer, *J. Phys. Chem. B*, 2004, **108**, 19912–19916.
13 X. Li, Y. Zhu, W. Cai, M. Borysiak, B. Han, D. Chen, R. D. Piner, L. Colombo and R. S. Ruoff, *Nano Lett.*, 2009, **9**, 4359–4363.
14 N. Peltekis, S. Kumar, N. McEvoy, K. Lee, A. Weidlich and G. S. Duesberg, *Carbon*, 2012, **50**, 395–403.
15 K. S. Novoselov and A. K. Geim, *Nat. Mater.*, 2007, **6**, 183–191.
16 D. R. Dreyer, S. Park, C. W. Bielawski and R. S. Ruoff, *Chem. Soc. Rev.*, 2010, **39**, 228–240.
17 S. Alwarappan, C. Liu, A. Kumar and C. Z. Li, *J. Phys. Chem. C*, 2010, **114**, 12920–12924.
18 K. Zhou, Y. Zhu, X. Yang and C. Li, *Electroanalysis*, 2010, **22**, 259–264.
19 X. Kang, J. Wang, H. Wu, I. A. Aksay, J. Liu and Y. Lin, *Biosens. Bioelectron.*, 2009, **25**, 901–905.
20 Z. Wang, X. Zhou, J. Zhang, F. Boey and H. Zhang, *J. Phys. Chem. Lett.*, 2009, **113**, 14071–14075.
21 K. R. Ratinac, W. Yang, J. J. Gooding, P. Thordarson and F. Braet, *Electroanalysis*, 2011, **4**, 803–826.
22 C. X. Lim, H. Y. Hoh, P. K. Ang and K. P. Loh, *Anal. Chem.*, 2010, **82**, 7387–7393.
23 W. Li, C. Tan, M. A. Lowe, H. D. Abruña and D. C. Ralph, *ACS Nano*, 2011, **5**, 2264–2270.
24 D. A. C. Brownson, M. G. Mingot and C. E. Banks, *Phys. Chem. Chem. Phys.*, 2011, **13**, 20284–20288.
25 D. A. C. Brownson, L. J. Munro, D. K. Kampouris and C. E. Banks, *RSC Adv.*, 2011, **1**, 978–988.
26 W. Gao, N. Singh, L. Song, Z. Liu, A. L. M. Reddy, L. J. Ci, R. Vajtai, Q. Zhang, B. Q. Wei and P. M. Ajayan, *Nat. Nanotechnol.*, 2011, **6**, 496–500.
27 V. Strong, S. Dubin, M. F. El-Kady, A. Lech, Y. Wang, B. H. Weiller and R. B. Kaner, *ACS Nano*, 2012, **6**, 1395–1403.
28 M. F. El-Kady, V. Strong, S. Dubin and R. B. Kaner, *Science*, 2012, **335**, 1326–1331.
29 H. Tian, Y. Shu, Y. L. Cui, W. T. Mi, Y. Yang, D. Xie and T. L. Ren, *Nanoscale*, 2014, **6**, 669–705.
30 D. A. C. Brownson, S. A. Varey, F. Hussain, S. J. Haigh and C. E. Banks, *Nanoscale*, 2014, **6**, 1607.
31 V. Nguyen, L. Tang and J.-J. Shim, *Colloid Polym. Sci.*, 2013, **291**, 2237–2243.
32 H. Wang, Y. Zhang, H. Li, B. Du, H. Ma, D. Wu and Q. Wei, *Biosens. Bioelectron.*, 2013, **49**, 14–19.
33 H. Song, Y. Ni and S. Kokot, *Anal. Chim. Acta*, 2013, **788**, 24–31.

34 R. Oprea, S. F. Peteu, P. Subramanian, W. Qi, E. Pichonat, H. Happy, M. Bayachou, R. Boukherroub and S. Szunerits, *Analyst*, 2013, **138**, 4345–4352.
35 S. Eissa, L. L'Hocine, M. Siaj and M. Zourob, *Analyst*, 2013, **138**, 4378–4384.
36 L. Wang, D. Lu, S. Yu, X. Shi, C. Wang and Y. Zhang, *J. Appl. Electrochem.*, 2013, **43**, 855–863.
37 A. Radoi, A. Obreja, S. V. Eremia, A. Bragaru, A. Dinescu and G.-L. Radu, *J. Appl. Electrochem.*, 2013, **43**, 985–994.
38 E. P. Randviir, D. A. C. Brownson, M. Gomez-Mingot, D. K. Kampouris, J. Iniesta and C. E. Banks, *Nanoscale*, 2012, **4**, 6470–6480.
39 R. S. Nicholson, *Anal. Chem.*, 1965, **37**, 1351–1355.
40 I. Lavagnini, R. Antiochia and F. Magno, *Electroanalysis*, 2004, **16**, 505–506.
41 A. T. Valota, I. A. Kinloch, K. S. Novoselov, C. Casiraghi, A. Eckmann, E. W. Hill and R. A. W. Dryfe, *ACS Nano*, 2011, **5**, 8809–8815.
42 V. C. Tung, M. J. Allen, Y. Yang and R. B. Kaner, *Nat. Nano*, 2009, **4**, 25–29.
43 W. S. Hummers and R. E. Offeman, *J. Am. Chem. Soc.*, 1958, **80**, 1339–1339.
44 M. F. El-Kady and R. B. Kaner, *Nat. Commun.*, 2013, **4**, 1475.